Probability Distribution of Majorana End-State Energies in Disordered Wires

Piet W. Brouwer, Mathias Duckheim, Alessandro Romito, and Felix von Oppen

Dahlem Center for Complex Quantum Systems and Fachbereich Physik, Freie Universität Berlin, 14195 Berlin, Germany

(Received 8 April 2011; published 1 November 2011)

One-dimensional topological superconductors harbor Majorana bound states at their ends. For superconducting wires of finite length L, these Majorana states combine into fermionic excitations with an energy ε_0 that is exponentially small in L. Weak disorder leaves the energy splitting exponentially small, but affects its typical value and causes large sample-to-sample fluctuations. We show that the probability distribution of ε_0 is log normal in the limit of large L, whereas the distribution of the lowest-lying bulk energy level ε_1 has an algebraic tail at small ε_1. Our findings have implications for the speed at which a topological quantum computer can be operated.

DOI: 10.1103/PhysRevLett.107.196804 PACS numbers: 73.63.Nm, 03.67.Lx, 71.23.−k

Introduction.—Quantum bits based on topologically protected states promise a platform for error-free quantum computation [1–3]. Since information is stored in states with a topologically protected degeneracy, qubits that rely on this principle are immune to local external sources of decoherence. In practical realizations, however, the energy splitting of the topological qubit is not exactly zero, because of finite-size effects. This poses a restriction on the speed at which a quantum computer must be operated. Operations have to be performed in a time that is short in comparison to the inverse energy splitting, but long in comparison to the inverse excitation gap for (nontopological) excitations.

A particularly promising possibility to realize topologically protected zero-energy states is found in one-dimensional spinless p-wave superconductors, which are known to have zero-energy Majorana fermion states at their ends [4,5]. Although Majorana excitations are insufficient to build a universal topological quantum computer, their implementation may considerably reduce the minimum required accuracy of qubit operations. There are several proposals for the experimental realization of such topological superconducting wires [6–11]. In some of these, one-dimensional wires can be brought into an alternation of topological and nontopological domains, with Majorana bound states at the domain boundaries [7,8,12], whose location can be controlled via gate voltages or magnetic fields [8,13].

Experimental realizations necessarily involve topological domains of finite length L, as well as disorder. For finite L, the Majorana end states fuse into fermionic excitations at a finite energy ε_0 that is exponentially small in L/ξ, where ξ is the superconductor coherence length [5]. In disordered wires, this sets a lower bound for the speed of qubit operations which is sample specific. On the other hand, disorder is known to cause a Lifschitz tail of localized states below the gap Δ [5,14]. Since operations with Majorana states require that they are transported through the quantum wires [13], the lowest-lying bulk state of energy ϵ_1 provides an upper bound for the speed of qubit operations. In view of possible experimental applications and their limitations, it is essential to know the full probability distribution of the energies ε_0 and ε_1. This problem is addressed in this Letter.

Models of topological superconductors.—We consider two models known to support Majorana end states. One model describes a one-dimensional, spinless p-wave superconductor [4,5],

$$H = \left(\frac{p^2}{2m} + V(x) - \mu\right)\sigma_z - \Delta' p \sigma_x. \tag{1}$$

Here, m is the mass, $\mu = p_F^2/2m$ the chemical potential, $p_F = m v_F$ the Fermi momentum, and σ_i denotes Pauli matrices in electron-hole space. The disorder potential $V(x)$ is drawn from a Gaussian distribution with zero mean and correlator $\langle V(x)V(x')\rangle = \gamma\delta(x - x')$, corresponding to the mean free path $l = v_F\tau = v_F^2/\gamma$ in the normal state. The superconducting gap $\Delta = \Delta' p_F = \hbar v_F/\xi$ is induced by proximity to a bulk superconductor so that Δ is not subject to a self-consistency condition. Throughout our calculation, we assume that $\xi, l \gg \hbar/p_F$.

A second model for a topological superconductor is the Dirac Hamiltonian with random mass,

$$H = v_F p \sigma_z - \Delta(x)\sigma_x - V(x)\sigma_x, \tag{2}$$

where Δ is an effective superconducting gap which changes sign at the topological phase transition in the absence of disorder. The Pauli matrices σ_i act in the space of right- and left-moving Majorana modes. The disorder potential $V(x)$ induces backscattering between these modes and thus appears as a random mass in Eq. (2). It is taken according to the same distribution as for the Hamiltonian (1). (Long-range correlated disorder which breaks the system into topological and nontopological regions has been considered in Refs. [15,16].)

Both of these Hamiltonians appear as effective models for a variety of physical systems. For instance, Eq. (1) describes semiconductor wires with strong spin-orbit

coupling in proximity to an s-wave superconductor in the limit of large applied magnetic field B [13,17]. Equation (2) appears in the same context when considering the vicinity of the topological phase transition in the clean limit. In this context, the effective gap Δ in Eq. (2) is the difference between the applied magnetic field B and the proximity-induced superconducting gap at $B = 0$ [17]. The Hamiltonian (2) also arises, e.g., for fermions on a lattice with random hopping [18], narrow-gap semiconductors [19,20], or organic molecules [21]. What appears here as a pair of Majorana end states is referred to as a "soliton–antisoliton pair" in these contexts [22].

Dirac equation with random mass.—We start by analyzing the end-state energies of the simpler Dirac Hamiltonian (2). To model a wire of finite length L we set $\Delta(x) \to -\infty$ for $x < 0$ and $x > L$ and $\Delta(x) = \Delta$ for $0 < x < L$. Since the system is fully gapped for $x < 0$ and $x > L$, any states contributing to the integrated density of states $N(\varepsilon) = \int_0^\varepsilon d\varepsilon' \nu(\varepsilon')$ must be localized in the interval $0 < x < L$. In the presence of disorder, $N(\varepsilon)$ is a random quantity with probability distribution $P_\varepsilon(N)$, which is related to the probability distribution $p_j(\varepsilon)$ of the energy level ε_j ($j = 0, 1, 2, \ldots$) through the equalities

$$p_j(\varepsilon) = -\frac{\partial}{\partial \varepsilon} \sum_{j'=0}^{j} P_\varepsilon(j'). \tag{3}$$

For each disorder configuration, we can calculate $N(\varepsilon)$ from the scattering matrix $S(\varepsilon, x')$ of a wire with Hamiltonian (2) for $x < x'$ and $H = v_F p \sigma_z$ for $x > x'$, see Fig. 1(a). The relation between $S(\varepsilon, x')$ (a complex number of unit modulus in the present case) and $N(\varepsilon)$ is given by the Friedel sum rule [23],

$$N(\varepsilon) = \frac{1}{2\pi i}\left\{\lim_{x' \to \infty} \ln \det[S(\varepsilon, x')] - \ln \det[S(\varepsilon, 0)]\right\}, \tag{4}$$

where the second term subtracts the contribution to the phase of det$S$ from scattering off the left half-infinite, fully gapped region ($\Delta \to -\infty$) with S matrix $S(\varepsilon, 0) = i$. We then proceed as follows to calculate $S(\varepsilon, x')$. From the Hamiltonian (2) we obtain the scattering matrix $\tilde{S}(\varepsilon, \delta x')$ of a slice of the wire with length $\delta x' \ll \min(l, \xi)$. Upon concatenating $S(\varepsilon, x')$ with $\tilde{S}(\varepsilon, \delta x')$, we obtain the evolution of $S(\varepsilon, x')$ with increasing x' [24]. This evolution has drift contributions due to the kinetic and pairing terms in Eq. (2), and a stochastic contribution from the disorder potential. It is a Langevin process, which takes its simplest form if we use the parametrization

$$S = i \tanh y, \tag{5}$$

where y takes values on the real axis $\pm i\pi/4$, see Fig. 1(b), and is continuous at $y = \pm\infty$. The Langevin process is specified by the equations

$$\langle \delta y \rangle = \frac{\delta x'}{v_F}[i\varepsilon \sinh 2y - \Delta(x')], \qquad \langle \delta y^2 \rangle = \frac{\delta x'}{l}. \tag{6}$$

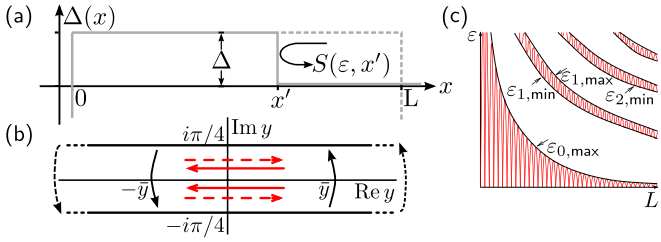

FIG. 1 (color online). (a) Pairing potential $\Delta(x)$ used for the calculation of the scattering matrix $S(\varepsilon, x')$ for $0 < x' < L$ (solid gray line) and for $x' > L$ (dashed). (b) The variable y in the parametrization (5) of the scattering matrix takes values on the real axis $\pm i\pi/4$. The black dotted arrows indicate the boundary conditions at $y = \pm\infty$. In the simplified Langevin process used for the asymptotic analysis (8), the boundary conditions are at Re$y = \pm\bar{y}$ (full black arrows). The direction of the drift term in topological ($0 < x' < L$) and nontopological ($x' < 0$ and $x' > L$) regions is indicated by the full red arrow and dashed red arrow, respectively. (c) Typical dependence of the Majorana end-state energy ε_0 and the energies $\varepsilon_1, \varepsilon_2, \ldots$, of low-lying bulk states on the system size L.

[The reason we used the unusual parametrization (5) is that it makes the noise term in Eq. (6) independent of S.] Near $y = \pm\infty$, the shifts are dominated by the term proportional to ε, which unidirectionally couples the branch at $y = \pm\infty \mp i\pi/4$ into the branch at $y = \pm\infty \pm i\pi/4$, see Fig. 1. The Langevin process has the initial condition $S(\varepsilon, 0) = i$ or, equivalently, $y = \infty + i\pi/4$ for $x' < 0$. Note that for $x' > L$, the Langevin process returns y to this starting point. The Friedel sum rule (4) now identifies $P_\varepsilon(N)$ as the probability distribution of the number of times N that the variable y has passed through the point at $-\infty$ upon increasing x' from $x' = 0$ to $x' = L$. We have calculated this probability distribution through direct numerical simulation of the Langevin process, as well as through an asymptotic analysis in the limit $\varepsilon \ll \min(\Delta, 1/\tau)$.

For the asymptotic analysis, we observe that the term proportional to ε dominates the Langevin process when

$$|\text{Re}y| \gtrsim \bar{y}(\varepsilon) = \frac{1}{2} \ln \frac{\max(2\Delta, 1/\tau)}{\varepsilon}. \tag{7}$$

The other terms dominate for $|\text{Re}y| \lesssim \bar{y}(\varepsilon)$. Thus, to logarithmic accuracy, we can reduce Eq. (13) to a truncated process in which $|\text{Re}y| < \bar{y}$ and the energy contribution to $\langle \delta y \rangle$ is omitted [25]. The unidirectional connection between the upper and lower branches now takes place at Re$y = \pm\bar{y}(\varepsilon)$, see Fig. 1(b). The resulting Langevin process for y is then specified by the equations

$$\langle \delta y \rangle = -\delta x'/\xi, \qquad \langle \delta y^2 \rangle = \delta x'/l, \tag{8}$$

with absorbing boundary conditions ("sink") at $y = \pm[\bar{y}(\varepsilon) - i\pi/4]$ and hard-wall boundary conditions at $y = \pm[\bar{y}(\varepsilon) + i\pi/4]$, see Fig. 1(b).

There is a qualitative difference between the Langevin processes at the upper branch (Im$y = \pi/4$) and the lower

branch (Im$y = -\pi/4$). At the upper branch, the drift term proportional to $1/\xi$ pushes the variable y towards the sink, whereas at the lower branch it keeps it away from the sink. The slow diffusion in the latter case does not affect ε_0, but it dominates the probability distribution of all higher levels ε_j, $j = 1, 2, \ldots$. By analyzing the diffusion process on the upper branch, we find that the probability $P_\varepsilon(0)$ is [26]

$$P_\varepsilon(0) = \frac{1}{2}\,\mathrm{erfc}\left(\frac{L/\xi - 2\bar{y}(\varepsilon)}{\sqrt{2L/l}}\right). \tag{9}$$

Using Eq. (3) and recalling that $\bar{y}(\varepsilon)$ is given by Eq. (7), we conclude that $\ln(\varepsilon_0/2\Delta)$ has a normal distribution with mean and variance given by

$$\langle \ln(\varepsilon_0/2\Delta)\rangle = -L/\xi, \qquad \mathrm{var}\ln(\varepsilon_0/2\Delta) = L/l, \tag{10}$$

up to corrections of order unity that cannot be determined from the above argument. Similarly, analyzing the diffusion process on the lower branch, we find $P_\varepsilon(0) + P_\varepsilon(1) = e^{-\langle N(\varepsilon)\rangle}$, where the disorder-averaged integrated density of states $\langle N(\varepsilon)\rangle \propto (L/\xi)(\varepsilon/\Delta)^{2l/\xi}$ [20,25], with proportionality constant that could not be determined from the asymptotic analysis. From this, we find that $p_1(\varepsilon) \propto (L\tau/\xi)(\varepsilon/\Delta)^{2l/\xi - 1}$ for small ε. The theoretical predictions are compared to numerical simulations of the Langevin process in Fig. 2.

One-dimensional spinless p-wave superconductor.—We now extend these results to the Hamiltonian in Eq. (1). Previous studies of lattice versions of the model (1) addressed the disorder-averaged density of states $\langle \nu(\varepsilon)\rangle$ in the limit $L \to \infty$ [5,14]. Using a strong-disorder renormalization group approach, Motrunich *et al.* showed that the model (1) is in a topological phase if the disorder strength

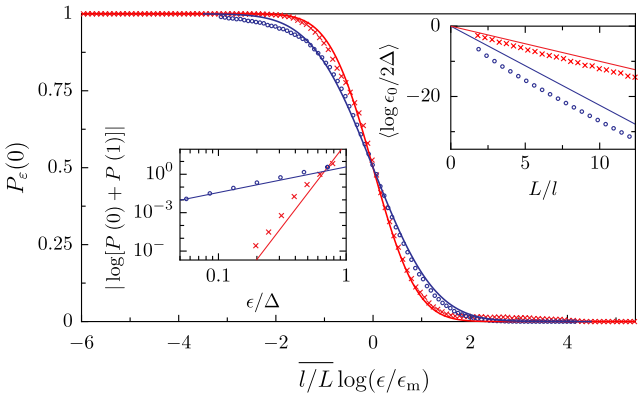

FIG. 2 (color online). Integrated probability density $P_\epsilon(0)$ of the Majorana end-state energies ε_0 (blue dots) and $\varepsilon_{0,\max}$ (red crosses) in the two models obtained from a numerical solution of the Langevin process, together with the theoretical prediction (solid). Energies are normalized to the median ϵ_m of the distribution. Left inset: Logarithm of the integrated probability distribution $P_\varepsilon(0) + P_\varepsilon(1)$ of the lowest-lying bulk state energies ε_1 and $\varepsilon_{1,\min}$. Right inset: Average of $\log\varepsilon_0$ and $\log\varepsilon_{0,\max}$ vs length. In both insets the slope of the solid lines is given by the theoretical predictions of the main text.

is below a critical value, and in a nontopological phase for stronger disorder. On both sides of the critical disorder strength, the density of states $\nu(\varepsilon)$ has a power law dependence on ε for $\varepsilon \ll \Delta$, with an exponent that depends on the disorder strength. For the continuum model (1) we now show that the transition is at $\xi = 2l$ and calculate the probability densities of the Majorana end-state energy ε_0 and the lowest-lying bulk level for disorder strengths below the critical value.

Our calculation essentially follows the approach taken above for the Dirac equation with random mass with some modifications. A wire of finite length L with hard-wall boundaries is modeled by setting $\mu = -\infty$ for $x < 0$ and $x > L$, and $\mu = p_F^2/2m > 0$ for $0 < x < L$ [27]. We define a 2×2 scattering matrix $S(\varepsilon, x')$ of a wire with Hamiltonian given by Eq. (1) for $x < x'$ and by $H = (p^2/2m)\sigma_z$ for $x > x'$ and parametrize S through

$$S(\varepsilon, x') = -\frac{1}{2}\sum_{\pm}\begin{pmatrix} \pm e^{i\phi}\tanh y_\pm & -i\tanh y_\pm \\ i\tanh y_\pm & \pm e^{-i\phi}\tanh y_\pm \end{pmatrix}, \tag{11}$$

where the variables y_+ and y_- take values on the real axis $\pm i\pi/4$, see Fig. 1, and ϕ is a real phase. The energy levels can no longer be calculated from the Friedel sum rule (4), but instead have to be obtained from the condition $\det[1 + S(\varepsilon, L)] = 0$, which becomes

$$\cos\phi = \coth(y_- - y_+) \tag{12}$$

in the parametrization (11). For $\hbar/p_F \ll \delta x' \ll l$, ξ, the resulting Langevin processes for the variables $y_\pm$ and the phase ϕ decouple,

$$\begin{aligned} \langle \delta y_\pm\rangle &= \frac{\delta x'}{v_F}(i\varepsilon \sinh 2y_\pm - \Delta) + \frac{\delta x'}{2l}\coth(y_\pm - y_\mp), \\ \langle \delta y_\pm^2\rangle &= -\langle \delta y_\pm \delta y_\mp\rangle = \delta x'/2l, \\ \langle \delta\phi\rangle &= 2p_F\delta x', \\ \langle \delta\phi^2\rangle &= 4\delta x'/l + (\delta x'/2l)\coth^2(y_+ - y_-). \end{aligned} \tag{13}$$

The initial condition is $\phi(0) = 0$ and $y_\pm(0) = \pm\infty \pm i\pi/4$. For a given disorder realization, the solutions ε_j of Eq. (12) oscillate as a function of L, with oscillation period $\approx \pi/p_F$, as shown schematically in Fig. 1(c). This follows from the observation that y_+ and y_- are "slow" as a function of L [they vary on the scale $\min(l, \xi)$], whereas ϕ is a "fast" variable ($\delta\phi/\delta x' \approx 2p_F$). Solutions of Eq. (12) then appear in quick succession upon increasing L at fixed ε, until y_+ passes through the point at $-\infty$ or y_- passes through the point at $+\infty$, whichever occurs first. No solutions of Eq. (12) are found upon increasing L further, until eventually again one of the variables $y_\pm$ passes through a point at infinity and solutions to Eq. (12) reappear in quick succession; cp. Fig. 1(c).

We now calculate the probability distributions $p_{0,\max}$ and $p_{1,\min}$ of the *maximum* $\varepsilon_{0,\max}$ and the *minimum* $\varepsilon_{1,\min}$ with respect to variations of L of order π/p_F. (Note that $\varepsilon_{0,\max}$ and $\varepsilon_{1,\min}$ are the energies relevant for setting the

operation speed of a hypothetical topological quantum computer.) Repeating the arguments of the first part of this Letter, these probabilities obey

$$p_{j,\max(\min)}(\varepsilon) = -\frac{\partial}{\partial\varepsilon}\sum_{j'\le 2j(j'\le 2j-1)} P_\varepsilon(j'), \qquad (14)$$

where $P_\varepsilon(N)$ is the probability that (in total) the variables y_+ or y_- have passed N times through the points at $\pm\infty$ upon increasing x' from 0 to L. We have calculated these probabilities from direct numerical simulation of the Langevin process, as well as from an asymptotic analytical solution valid in the limit $\varepsilon \ll \min(\Delta, 1/\tau)$. For the asymptotic analysis, we make the same simplification of the Langevin process as in the case of the Dirac equation with random mass. In addition, we observe that for the energies of interest, one of the variables $y_\pm$ effectively remains pinned at $-\bar{y}(\varepsilon) - i\pi/4$, so that the factor $\coth(y_+ - y_-)$ in the interaction term may be approximated by ± 1. The resulting Langevin process for the remaining variable is then specified by the equations

$$\langle \delta y\rangle = -\delta L/\xi + \delta L/2l, \qquad \langle \delta y^2\rangle = \delta L/2l, \qquad (15)$$

with the boundary conditions as specified below Eq. (8). The result for $P_\varepsilon(0)$ has the same functional form as in the case of the random-mass Dirac equation, and we conclude that $\ln(\varepsilon_{0,\max}/2\Delta)$ has a normal distribution with mean and variance given by

$$\begin{aligned} \langle \ln(\varepsilon_{0,\max}/2\Delta)\rangle &= -L[1/\xi - 1/(2l)], \\ \operatorname{var}\ln(\varepsilon_{0,\max}/2\Delta) &= L/2l, \end{aligned} \qquad (16)$$

up to corrections of order unity that cannot be determined from the asymptotic argument. The end-state energy remains exponentially small in L as long as $2l > \xi$, which identifies $2l = \xi$ as the critical disorder strength that drives the system into the nontopological phase. Similarly, we find $P_\varepsilon(0) + P_\varepsilon(1) = e^{-\langle N(\varepsilon)\rangle}$, with $\langle N(\varepsilon)\rangle \propto (L/\xi)\times(\varepsilon/\Delta)^{4l/\xi-2}$ [5,14,25], from which we conclude that $p_{1,\min}(\varepsilon) \propto (L\tau/\xi)(\varepsilon/\Delta)^{4l/\xi-3}$ for small energies. At the critical disorder strength, the integrated density of states takes the Dyson form $N(\varepsilon, L) \propto \ln^2(\varepsilon/\Delta)$ [5,14,28]. The theoretical prediction for $p_{0,\max}$ is compared to numerical simulations of the Langevin process in Fig. 2.

Conclusions.—For both models of a topological superconducting wire, we find that the energy splitting ε_0 of the Majorana end states has a log-normal distribution, implying large sample-to-sample fluctuations. Nevertheless, for sufficiently long wires, the width of the log-normal distribution remains small compared to its average. In this case, the lower limit on the speed of the qubit operations is well determined by the typical value of the log-normal distributions in Eqs. (10) and (16), which is exponentially small in L/ξ. By contrast, we find that the energy ε_1 of the lowest-lying bulk state is algebraically small in L/ξ. This implies that in principle, there is a large parameter window in which both conditions on the operation speed can be met if L is made sufficiently large. It is important to note, however, that with increasing disorder or increasing L, this parameter window is shifted to lower energies which would require the topological quantum computer to operate at a lower temperature and lower speed.

This work is supported by the DFG through SPP 1285 and the Alexander von Humboldt Foundation.

[1] A. Y. Kitaev, Ann. Phys. (N.Y.) **303**, 2 (2003).
[2] M. H. Freedman, Proc. Natl. Acad. Sci. U.S.A. **95**, 98 (1998).
[3] C. Nayak, S. H. Simon, A. Stern, M. Freedman, and S. Das Sarma, Rev. Mod. Phys. **80**, 1083 (2008).
[4] A. Y. Kitaev, Phys. Usp. **44**, 131 (2001).
[5] O. Motrunich, K. Damle, and D. A. Huse, Phys. Rev. B **63**, 224204 (2001).
[6] J. D. Sau, R. M. Lutchyn, S. Tewari, and S. Das Sarma, Phys. Rev. Lett. **104**, 040502 (2010).
[7] R. M. Lutchyn, J. D. Sau, and S. Das Sarma, Phys. Rev. Lett. **105**, 077001 (2010).
[8] Y. Oreg, G. Refael, and F. von Oppen, Phys. Rev. Lett. **105**, 177002 (2010).
[9] A. C. Potter and P. A. Lee, Phys. Rev. Lett. **105**, 227003 (2010).
[10] M. Duckheim and P. W. Brouwer, Phys. Rev. B **83**, 054513 (2011).
[11] S. B. Chung, H.-J. Zhang, X.-L. Qi, and S.-C. Zhang, Phys. Rev. B **84**, 060510 (2011).
[12] L. Fu and C. L. Kane, Phys. Rev. Lett. **100**, 096407 (2008).
[13] J. Alicea, Y. Oreg, G. Refael, F. von Oppen, and M. P. A. Fisher, Nature Phys. **7**, 412 (2011).
[14] I. A. Gruzberg, N. Read, and S. Vishveshwara, Phys. Rev. B **71**, 245124 (2005).
[15] V. Shivamoggi, G. Refael, and J. E. Moore, Phys. Rev. B **82**, 041405 (2010).
[16] K. Flensberg, Phys. Rev. B **82**, 180516 (2010).
[17] P. W. Brouwer, M. Duckheim, A. Romito, and F. von Oppen, arXiv:1103.2746 [Phys. Rev. B (to be published)].
[18] T. P. Eggarter and R. Riedinger, Phys. Rev. B **18**, 569 (1978); G. Theodorou and M. H. Cohen, Phys. Rev. B **13**, 4597 (1976).
[19] L. V. Keldysh, Zh. Eksp. Teor. Fiz. **45**, 364 (1963).
[20] A. A. Ovchinnikov and N. S. Érikhman, Zh. Eksp. Teor. Fiz. **73**, 650 (1977) [Sov. Phys. JETP **46**, 340 (1977)].
[21] K. Kim, R. H. McKenzie, and J. W. Wilkins, Phys. Rev. Lett. **71**, 4015 (1993).
[22] A. J. Heeger, S. Kivelson, J. R. Schrieffer, and W. P. Su, Rev. Mod. Phys. **60**, 781 (1988).
[23] A. C. Hewson, *The Kondo Problem to Heavy Fermions* (Cambridge University Press, Cambridge, 1997).
[24] C. W. J. Beenakker, Rev. Mod. Phys. **69**, 731 (1997).
[25] P. W. Brouwer, C. Mudry, and A. Furusaki, Phys. Rev. Lett. **84**, 2913 (2000).
[26] M. V. Smoluchowski, Phys. Z. **17**, 557 (1916).
[27] N. Read and D. Green, Phys. Rev. B **61**, 10 267 (2000).
[28] M. Titov, P. W. Brouwer, A. Furusaki, and C. Mudry, Phys. Rev. B **63**, 235318 (2001).